Applied Surface Science 644 (2024) 158791

Contents lists available at ScienceDirect

Applied Surface Science

journal homepage: www.elsevier.com/locate/apsusc

Full Length Article

Increasing the thermal stability of a Cr/Sc multilayer by nitriding

E.O. Filatova [a,*], S.S. Sakhonenkov [a], A.V. Solomonov [a], R.M. Smertin [b], V.N. Polkovnikov [b]

[a] Institute of Physics, St-Petersburg State University, Ulyanovskaya Str. 1, Peterhof, St. Petersburg 198504, Russia
[b] Institute for Physics of Microstructure, Russian Academy of Sciences, Nizhny Novgorod 603087, Russia

ARTICLE INFO

Keywords:
Multilayer
Cr/Sc
Layer intermixing
Nitriding
Thermal stability

ABSTRACT

The effect of nitridation of Cr, Sc or both layers in the ultrathin multilayer structure Sc/Cr on the intermixing of thin Cr and Sc layers, as-deposited and after annealing at different temperatures were considered in details. The processes of passivation by nitrogen and synthesis in nitrogen medium of chromium and scandium layers are also compared. It was established that during passivation process the nitrogen interacts with surface of scandium film forming a ScN_x compound and does not interact at all with the chromium layer. A net scavenging of nitrogen is observed in the case of CrN_x/Sc system, while in the Sc/CrN_x system the interaction of scandium with nitrogen gas before chromium layer deposition with formation of some amount of ScN_x is added.

Based on theoretical analysis of the effect of nitriding the system and detailed analysis carried out by photoelectron spectroscopy a multilayer system $[Sc/CrN_x]_{300}$ was synthesized and analyzed at different temperatures of annealing. Analysis of X-ray diffraction data showed that the sample consists of X-ray amorphous layers, the crystallinity of which practically does not change with increasing temperature. The results show that the $[Sc/CrN_x]_{300}$ system with small nitrogen content is very resistant to elevated temperatures up to 450 °C.

1. Introduction

Today, there is no doubt that the mixing of layers at the interfaces between two materials due to interdiffusion and chemical reactions including oxygen and nitrogen redistribution during synthesis is the main driving force for the formation of an interfacial barrier, which effects on different characteristics of the structures: effective work function [1–10] as well as the reflection coefficient of multilayer structures [11–17] and some others. At the same time the atomic pattern of this important process and the most effective ways to deal with it remains incomplete. Thus, in the case of multilayer X-ray mirrors the most of the attention so far has been devoted to the processes of formation of interlayer roughness, which leads to a change in the extension of the transition region while the formation of new compounds, as well as their effect on the sharpness of the interface, has received less attention. This problem is particularly acute in the case of multilayer systems with thin layers (thickness smaller than 1 nm).

Owing to mechanical [18–21], plasmon [22], piezoelectric [23–25], and thermoelectric properties [26], thin films of transition metal and transition metal nitride are widely studied for effective application in multilayer coatings with superior mechanical and tribological properties, microelectronics, X-ray optics and some other.

Significant progress in recent years in the development of multilayer coatings in the extreme ultraviolet (EUV) region is undoubtedly determined by the achievements in the development of EUV lithography for the semiconductor industry, which are to some extent determined by the search and application of new advanced technologies for smoothing interfaces. Roughness and/or interdiffusion of materials in multilayer structures is the main reason for the sharp decrease in the reflectivity of the coating in this region. From the point of view of such fields of knowledge as materials science, biology, and medicine, the wavelength range of the water window is of particular interest [27–38]. Systems based on Cr/Sc, consisting of layers with a thickness of less than 1 nm, demonstrate the most promising combination of materials for this range. Despite the high theoretical reflectivity (64%) of a short-period Cr/Sc mirror at an energy of 398 eV and normal incidence angle, the experimental values of its reflectivity are much lower [39,40]. Various methods have been tried by various groups to improve the efficiency of the Cr/Sc mirror, including barrier layer technology [41,42], substrate bias voltages [43], the introduction of O and N impurities during the deposition process [42,44,45].

As follows from the works [42,46,47], the deposition of a B_4C barrier layer on the chromium layer or onto both layers (chromium and scandium) protects the crystallization process in the structure and

* Corresponding author.
E-mail address: e.filatova@spbu.ru (E.O. Filatova).

https://doi.org/10.1016/j.apsusc.2023.158791
Received 13 September 2023; Received in revised form 19 October 2023; Accepted 28 October 2023
Available online 31 October 2023
0169-4332/© 2023 Elsevier B.V. All rights reserved.

demonstrates a higher reflectivity. Also, a better thermal stability as compared to Cr/Sc multilayers was traced. In our recent work [48], it was shown that the introduction of a Si barrier layer between scandium and chromium makes it possible to preserve the amorphous structure up to a temperature of 450 °C.

A special attention was paid to another method of the influence on the interface that can improve it and, as a consequence, increase the reflection coefficient and the thermal stability of short-period Cr/Sc structures. Ghafoor et al. have reported [45] that incorporation of N impurities during the deposition process effects on the interface quality reducing the interdiffusion that leads to more abrupt interfaces. However, this effect was established only for a small number of periods. Ericson et. al. [46] studied the Cr/Sc multilayers with 34 at.% incorporated nitrogen. They have shown that such system is a less perfect compared to the pure Cr/Sc: two slightly different periodicities was found in the system. Moreover, it was established that the period of the structure expands during annealing process. Inevitably, the question arises about the optimal nitrogen content in the layer, as well as the efficiency of nitriding one (Cr or Sc) or both layers. Further analyses of the interfaces in nitrided Cr/Sc multilayer structures would be required for a better understanding whether there are advantages in terms of thermal stability of the system due to the inclusion of nitrogen in Cr/Sc multilayers.

The aim of this work was to study the effect of nitridation of Cr or Sc or both layers on the intermixing of thin Cr and Sc layers, as-deposited and after annealing at different temperatures.

2. Experimental part

All samples were synthesized by DC magnetron sputtering. Detailed description of the equipment can be found in the works [49,50]. Nitriding was carried out by injection of nitrogen gas into the synthesis chamber during or after (in case of a layer passivation) material deposition. The partial pressure of N_2 ranged from 3% to 20% relative to the Ar gas pressure of 0.1–0.13 Pa. The pressure was measured by utilizing Pfeiffer PKR 251. The purity of the nitrogen gas was 99.998%, and the argon gas was 99.998%. Targets of Cr, Sc, Be and B_4C were used for sputtering. They represented disks of 150 mm in diameter and 5 mm in thickness. Si wafers with super-polished surface whose RMS roughness was no worse than 0.2 nm were used as substrate. The parameters of synthesis, such as magnetron voltage, discharge current, residual gas pressure and evaluated thicknesses of layers in the samples are presented in Table S1. Evaluation of the actual layer thicknesses was performed by fitting experimental X-ray reflection curves obtained at an X'Pert PRO MRD diffractometer (PANAlitical, Netherlands, 2006).

X-ray photoelectron spectra were measured at two spectrometers: ESCALAB 250 Xi of the "Centre for Physical Methods of Surface Investigation" of the Research Park, Saint-Petersburg State university; ESCA laboratory module at the NANOPES station of the National Research Center "Kurchatov institute". Both spectrometers are equipped with an X-ray source with an energy of 1486.6 eV and have comparable energy resolution. More detailed information about parameters of the laboratory stations can be found elsewhere [48]. Annealing of the samples was performed in the preparation chamber of the ESCALAB Xi 250 spectrometer in high vacuum (residual gas pressure was approximately 10^{-6} Pa).

To carry out a detailed analysis, the photoelectron spectra were decomposed into their constituent components. To ensure the reliability of the resulting decompositions, the peak parameters were set based on the parameters obtained for the lines in the spectra of the reference samples. For ease of comparison, in some figures the background of inelastically scattered photoelectrons is subtracted from the spectra, and normalization is also carried out to the maximum intensity of the photoelectron line. The background was set using the universal Tougaard function [51]. To establish the main parameters of photoelectron lines (shape and energy position), the spectra of reference samples Sc, Cr, ScN_x and CrN_x were measured. During the decomposition of complex systems, the positions of peaks other than ScN_xO_y were fixed.

3. Results and discussion

3.1. Interaction of chromium and scandium with nitrogen

To understand the processes occurring between the Cr and Sc layers during nitriding of one of them or both layers, at the first stage, we considered the interaction of nitrogen with each of these layers separately. Fig. 1a displays the detailed photoelectron spectrum of the Sc 2p core level together with the deconvoluted peaks for thick scandium film. Five peaks were introduced to perform the decomposition procedure of this spectrum. Sc $2p_{3/2}$ peaks originating from pure scandium and scandium oxide are centered at 398.3 eV and 402.0 eV, respectively, and is in good agreement with the literate values [52]. It should be noted that the Sc 2p spectrum is characterized by a doublet structure, which is a consequence of the spin–orbit splitting, the value of which is 4.7 ± 0.2 eV [52], the intensity ratio of Sc $2p_{3/2}$ and Sc $2p_{1/2}$ is constrained to 2:1, which is in good agreement with the expected ratio of $(2j_1 + 1)/(2j_2 + 1)$, where j_1 and j_2 represent the total angular momentum quantum numbers for corresponding states of the unpaired core electron after the photoionization event. The fifth peak is a low intensity peak located at 396.6 eV, which can be assigned to a nitrogen 1s line [53].

It is important to note that scandium strongly interacts with all gases present in the magnetron sputtering plant that especially demands the minimal content of any impurities in the working gas before film deposition. Nevertheless, the low intensity nitrogen line found in the spectrum indicates the presence of nitrogen in the sample, which is apparently due to the presence of an insignificant amount of N_2 in the magnetron chamber before deposition of the film. Minor amounts of residual gases such as C, N and O have been found in Cr/Sc multilayer mirrors deposited under high vacuum by magnetron sputtering [45].

Fig. 1b shows the combined photoelectron spectrum of the Sc 2p and N 1s lines of the reference ScN_x film. Sc $2p_{3/2}$ peaks originating from ScN_x and ScN_xO_y are centered at 400.2 eV and 402.5 eV [54], respectively. A rather intense N 1s peak, which can be assigned to ScN_x, is located at lower energies (395.9 eV) compared to the nitrogen in the sample of metallic Sc film. And low intensity N 1s peak in the form of a shoulder located at a higher binding energy of 397.1 eV refers to the oxynitride ScN_xO_y [54].

Fig. 2a displays the measured and fitted Cr 2p photoelectron spectrum of reference Cr film. In contrast to numerous publications [55–59], we use the multiplet splitting of the Cr(III) compound in the decomposition of the spectrum, which is well confirmed experimentally [60–63].

Multiplet splitting occurs when an atom contains unpaired electrons. In this case, when a core electron vacancy is formed as a result of photoionization process, a bond can arise between the unpaired electron in the core and the unpaired electron in the outer shell. This can create a series of final states, which will show up in the photoelectron spectrum. Cr(III) contains three unpaired d electrons. Fitting parameters for Cr $2p_{3/2}$ spectra are based on spectra taken from a series of well-characterized standard compounds [62,64,65]. Cr(III) oxide shows discrete multiplet structure whereas the hydroxide shows only a broad peak shape (multiplet splitting is irresolvable). The decomposition carried such way allowed us to establish parameters of the chromium line (the energy position, lineshape and full width at half maximum). The narrow peak centered at (574.3 eV) can be attributed to metallic chromium [65].

Consideration of the decomposed Cr 2p spectrum of the CrN_x reference film draws attention to the fact that, in contrast to the spectrum of the ScN_x film, the spectrum of the nitride Cr film (Fig. 2b) contains a peak of metallic chromium in addition to the peak corresponding to the CrN_x compound. The chromium peaks (Cr $2p_{3/2}$) originating from metallic Cr, CrN_x and CrN_xO_y are centered at (574.3 eV), (575.4 eV) and (576.4 eV), respectively. N 1s spectrum, shown in the Fig. 2c consists

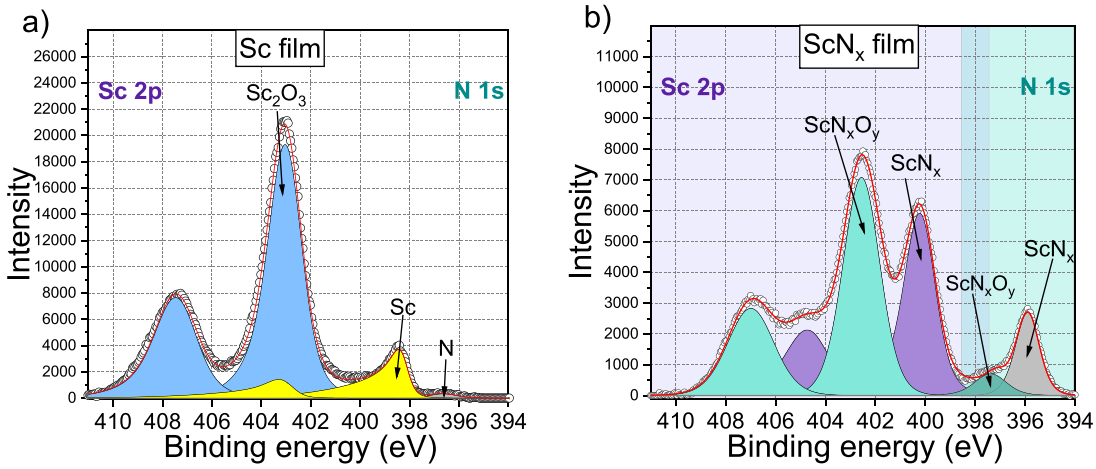

Fig. 1. Experimental and decomposed Sc 2p + N 1s photoelectron spectra collected from the a) Sc and b) ScN_x reference films.

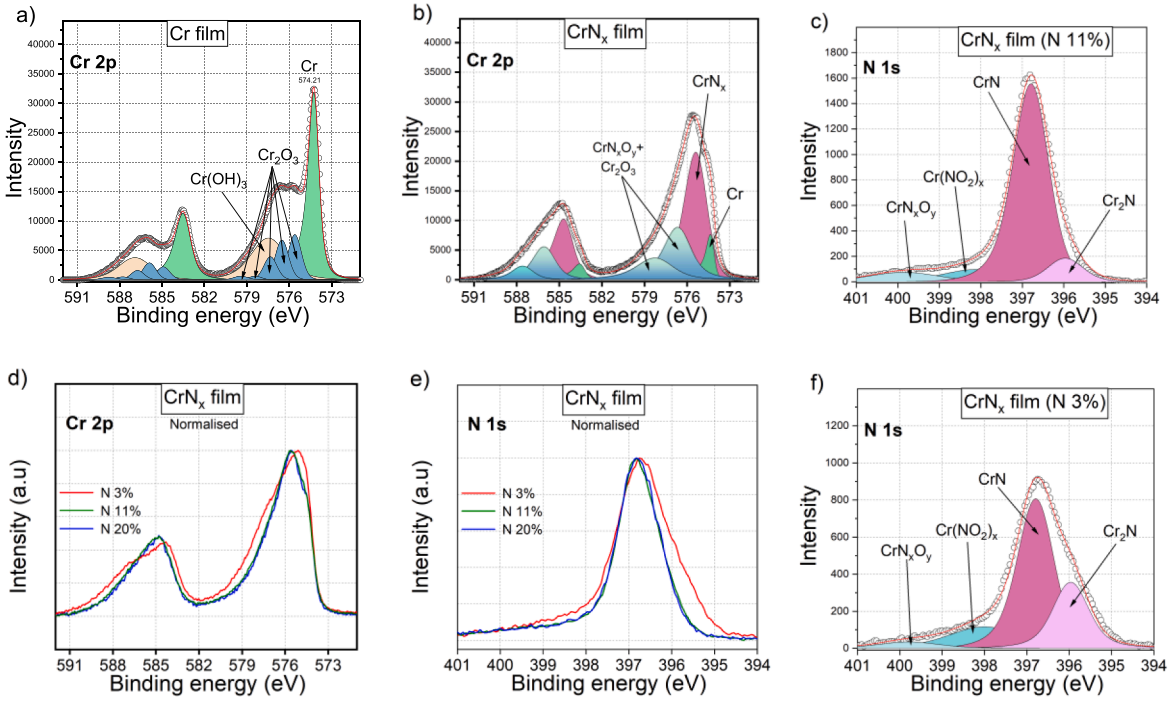

Fig. 2. Cr 2p and N 1s photoelectron spectra collected from the reference films Cr (a) and CrN_x (b)-(f). (b) and (c) figs. show the experimental and decomposed spectra of CrN_x film synthesized in an argon + nitrogen (11%) medium. (d) and (e) show the comparison of the spectra of three CrN_x films depending on the nitrogen partial pressure (3% or 11% or 20%). (d) shows the experimental and decomposed spectra of CrN_x film synthesized in an argon + nitrogen (3%).

from three peaks, which can be assigned to two different nitrides CrN (396.8 eV,) and Cr_2N (395.96 eV) [66]; tightness from the side of high energies is responsible for formation of the CrN_xO_y. Due to the proximity of the CrN and Cr_2N peaks relative to each other, it is not possible to separate them in the Cr 2p spectrum. Due to the complexity of decomposing a multicomponent spectrum using multiplet splitting and taking into account the overlap of individual components belonging to different compounds, we will further represent the components related to CrN_xO_y and Cr_2O_3 as total peaks.

Fig. 2d allows one to compare the Cr 2p spectra of CrN_x films synthesized in an argon atmosphere with different nitrogen contents. It should be noted that all three spectra in this case were measured at the station ESCALAB. For the convenience of comparison, the spectra are normalized to the intensity of Cr 2p peak. A joint analysis of the spectra indicates the effect of the nitrogen content on the ratio of the contributions of metallic chromium and CrN_x, as well as the effect of the nitrogen content on film oxidation. It can be seen that nitrogen protects the film from oxidation by environment oxygen to some extent: the higher the nitrogen content, the lower the oxidation process. It is interesting to note that, starting from nitrogen partial pressure of 11%, a further increase in its content does not affect the structure of the film: while a small amount of metallic chromium is retained in the film.

Also, it should be noted that according to N 1s spectra with an increase in the nitrogen content, the contribution of the Cr_2N component decreases significantly (Fig. 2c, f).

Fig. 3a,b displays the detailed photoelectron spectra of the Sc 2p + N 1s and Cr 2p core levels, together with the deconvoluted peaks collected from the Sc/N_2 and Cr/N_2 systems. In contrast to the ScN_x (CrN_x) film, which was deposited in the argon + nitrogen medium, in the Sc/N_2 (Cr/N_2) sample, nitrogen is supplied to the installation after the deposition of

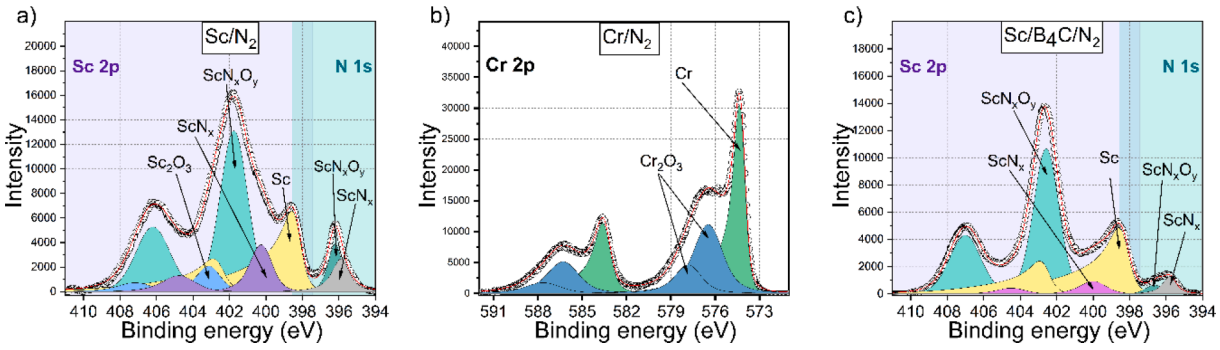

Fig. 3. Experimental and decomposed photoelectron spectra collected from the a) Sc/N_2, b) Cr/N_2 and c) $Sc/B_4C/N_2$ systems.

the Sc(Cr) film. That means the nitrogen is applied to an already deposited Sc(Cr) film. The joint analysis of the Sc 2p and Cr 2p photoelectron spectra allows us to conclude that the presence of nitrogen in the chamber leads to its interaction with surface of scandium film forming a ScN_x compound; at the same time nitrogen does not interact at all with the chromium layer. The last statement is confirmed by measured nitrogen spectra, which are not shown. A comparison of the spectra of Sc/N_2 and ScN_x indicates the interaction of nitrogen with scandium layer, leading to the formation of ScN_x while retaining a sufficient amount of metallic scandium. An intense peak located at the binding energy of 401.9 eV can be assigned to the formed oxynitride. The shift of this peak towards lower binding energies relative to the analogous peak in the ScN_x system by about 0.8 eV suggests a decrease in the oxygen content in the scandium oxynitride due to oxygen scavenging by scandium with the formation of scandium oxide. This assumption is confirmed by the presence of an Sc_2O_3 peak in the spectrum. It also should be noted that the contribution of oxynitride in the case of the Sc/N_2 system is significantly higher compared to the ScN_x system. Recall, that in both cases, i.e., both in the synthesis of sample ScN_x and in the synthesis of sample Sc/N_2, the same amount of nitrogen was used: the synthesis was carried out in an argon + nitrogen (11%) medium. It can be concluded that scandium actively interacts with nitrogen, regardless of the moment of nitrogen injection in the synthesis chamber. Nevertheless, passivation of the surface of the scandium film makes it possible to preserve the layer of metallic scandium from oxidation in the environment.

To limit the interaction of Sc layer with nitrogen medium a capping layer can be used. An example would be the $Sc/B_4C/N_2$ system with thin B_4C barrier layer. It should be noted that nitrogen was supplied after the deposition of the B_4C layer, but before the deposition of scandium for ~10 sec. Analysis of the detailed photoelectron spectrum of the Sc 2p + N 1s core levels reveal a significant decrease in the contribution of ScN_x and scandium oxynitride.

3.2. Estimation of layer thicknesses

Analysis of the Sc 2p spectra of the Sc and ScN_x films showed the presence of intense oxide peaks because of the formation of natural oxides. Since the thickness of the Sc layers in a multilayer is less than 1 nm, an assessment of the part of the layer that is oxidized is necessary. The evaluation of the thickness of natural oxides was carried out as follows. At the first stage of calculations, we consider two samples (both synthesized by magnetron sputtering and deposited on a silicon substrate) 40-nm-thick scandium film and 40-nm-thick scandium nitride film. The density of thin films may differ from the density of the bulk material, usually the difference is estimated at 5–10%. The values of density were taken from the CRC Handbook of Chemistry and Physics [67]. When determining the error in calculating the thickness of the surface layer, we assume that:

- density determination error is 5%;
- IMFP calculation error by TPP-2 M formula is 10%;
- the error in determining the molar mass and the emission angle is negligible.

The error in determining the intensity of the photoelectron peak will be estimated on the basis of Monte Carlo calculations in the CASAXPS program [68].

The thickness of the surface layer can be determined by the formula [69]:

$$d = \lambda_A \cdot \cos\theta \ln\left(1 + \frac{R}{R^\infty}\right)$$

$$R = \frac{I_A}{I_B}$$

$$R^\infty = \frac{n_A \lambda_{A,A}}{n_B \lambda_{B,A}} = \frac{\rho_A \lambda_{A,A} M_A}{\rho_B \lambda_{B,A} M_B}$$

where d is the thickness of the natural oxide surface layer, $I_{A,B}$ is the intensity of the photoelectron peak related to the material A of the layer or B of the substrate, n is the atomic concentration, M is the molar mass, ρ is the density, λ is the mean free path of inelastically scattered photoelectrons emitted from material *1* and propagating in material *2*, θ is the angle of photoelectron emission, R^∞ is the ratio of photoelectron peak intensities for the case of thick materials A and B. We assume that $\lambda_{A,A} \approx \lambda_{B,A}$.

The formation of an oxide layer on the surface leads to a change in the thickness of the initial layer that participated in the reaction. To estimate the layer broadening factor (Billing-Bedworth coefficient), we use the following formula:

$$\alpha = \frac{V_{ox}}{V_{me}} = \frac{M_{ox}\rho_{me}}{k \cdot M_{me}\rho_{ox}}$$

where M is the relative molecular weight, ρ is the density, *ox*, *me* are oxide and metal, respectively, k is the number of metal atoms in the oxide "molecule". If $\alpha > 1$, then a continuous layer of oxide film is formed. If $\alpha < 1$, then a porous layer of oxide film is formed. For both materials (Sc and ScN) the Sc 2p photoelectron spectra were used.

If we assume the formation of an oxide film on the surface of scandium, then the thickness of the surface layer of scandium oxide can be estimated as 5.0 nm ± 0.7 nm. By analogy, the thickness of the surface layer of scandium oxynitride is estimated as 2.3 nm ± 0.7 nm.

The thickness of the starting material that was oxidized was also evaluated. First, the broadening coefficient, which shows how thick the layer is formed if 1 nm of the starting material is oxidized. For Sc → Sc_2O_3 and ScN → $Sc_6N_2O_5$ was calculated. The broadening coefficients for Sc - Sc_2O_3 and ScN - $Sc_6N_2O_5$ were obtained as 1.19 and 1.15, respectively. The final assessment of the layer thicknesses gave the following values: the thickness of original Sc film, which was involved in

the process of oxidation is 4.2 nm ± 0.6 nm, the thickness of formed $Sc_6N_2O_5$ is 2.2 nm ± 0.6 nm. It can be seen that the thickness of the oxidized Sc (ScNx) in the 40 nm thick film is greater than the initial thickness of the Sc layer in a multilayer. This might be a reason to use Cr as a top layer in a multilayer.

3.3. Effect of layers ordering

Let us turn to the consideration of systems in which one of the layers (Cr or Sc) is nitrided and moreover we will analyze the effect of the ordering of the layers on the formation of the interface in these systems.

Fig. 4 displays the detailed Sc 2p + N1s and Cr 2p photoelectron spectra together with the peak fitting for the CrN_x(39 nm)/Sc(2 nm) and Sc(40 nm)/CrN_x(1 nm)/Be(1 nm) systems. A thin layer of beryllium was used to protect CrN_x layer from oxidation. Previously, we have shown that a beryllium layer with a nominal thickness of 1 nm on the tungsten surface is completely oxidized, forming a beryllium oxide film [70]. The formed BeO acts as a protective layer and prevents the oxidation of tungsten [71]. However, usage of the BeO overlayer on the scandium film is not effective since the Sc oxide has less formation energy (-3.97 eV/atom for Sc_2O_3 and -3.1 eV/atom for BeO) [67,72] and the scandium will interact with BeO. First, it should be paid attention to the film deposition process. In the CrN_x/Sc system, the growth of the CrN_x layer occurs in the Ar + N_2 medium. Before deposition of scandium, the nitrogen supply is turned off. The growth of the scandium layer occurs in the absence of nitrogen supply to the chamber. In the case of the synthesis of the Sc/CrN_x/Be system, nitrogen is supplied to the chamber almost immediately after the deposition of scandium to form a CrN_x layer. This means that during the deposition of the first atoms of the CrN_x film onto Sc, scandium may interact with nitrogen and some amount of ScN_x can be formed.

The detailed Sc 2p + N1s and Cr 2p photoelectron spectra for the CrN_x/Sc is shown in the Fig. 4 a,b. Analysis of the Cr 2p spectrum (Fig. 4b) reveals the presence of both CrN_x and metallic Cr compounds. Nevertheless, a joint analysis of the Cr 2p and Sc 2p spectra indicates a strong scavenging of nitrogen by scandium from the CrN_x layer. If the ratio of metallic chromium to CrN_x in the CrN_x reference film is 1:5 (0.2), then in the system CrN_x/Sc this ratio increases to value 8:5 (1.7).

Sc 2p spectrum examination traces a small ScN_x peak and a high intensity ScN_xO_y oxynitride component. (Fig. 4a). The position of the ScN_xO_y peak coincides with the position of the oxynitride in the spectrum of the ScN_x reference film. It should also be noted that Sc passes oxygen into the underlying layer of CrN_x, which leads to the formation of a small amount of chromium oxide.

Fig. 4c,d displays the Sc 2p + N1s and Cr 2p photoelectron spectra collected from the Sc(40 nm)/CrN_x(1 nm)/Be(1 nm) system. A detailed analysis of the Cr 2p spectrum of the Sc/CrN_x/Be system together with the CrN_x/Sc system indicates that in terms of a shape of the spectrum (number of details and their energy position) these spectra correlate well with each other. Nevertheless, the nitrogen scavenging by scandium

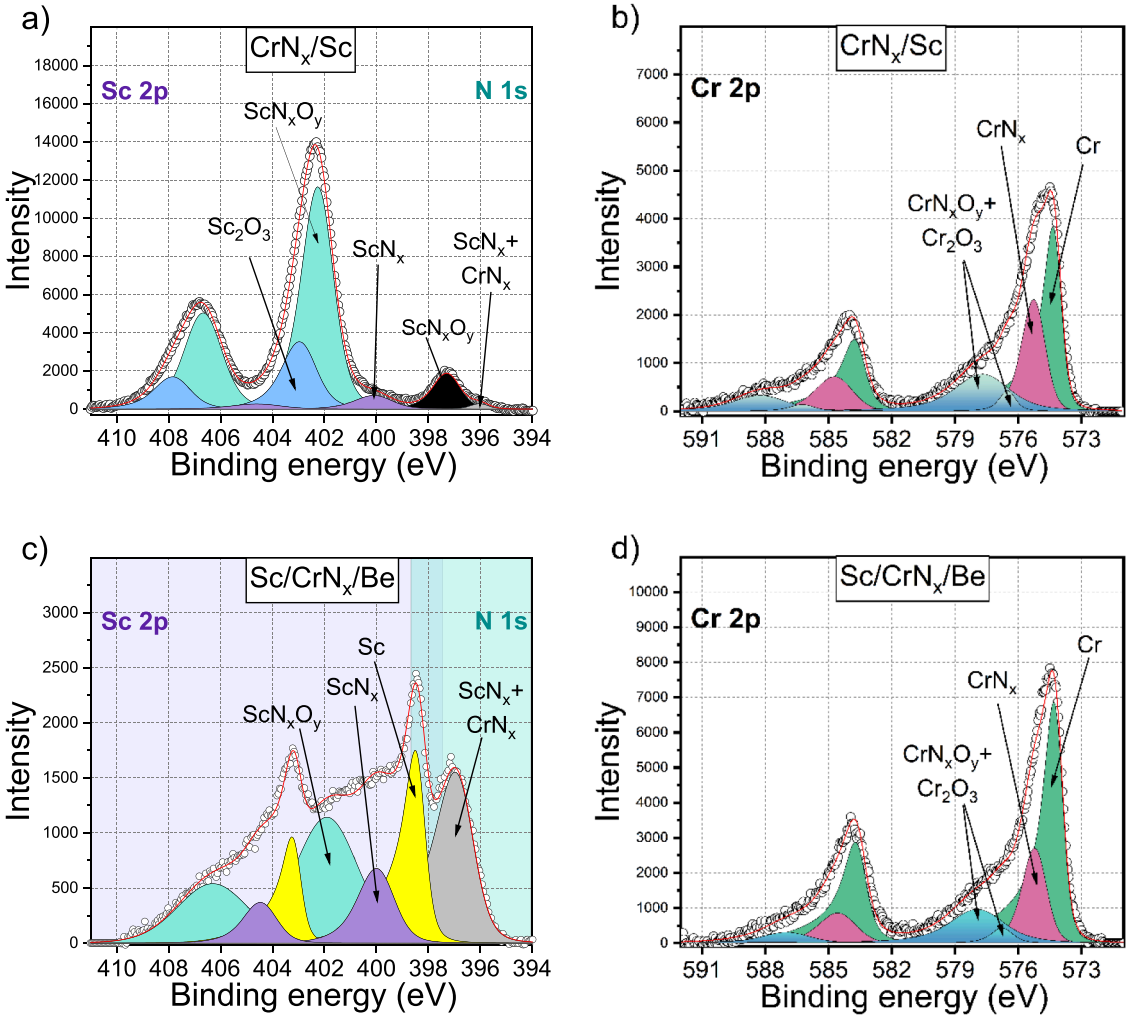

Fig. 4. Experimental and decomposed Sc 2p + N1s and Cr 2p photoelectron spectra collected from the CrN_x(39 nm)/Sc(2 nm) system (a), (b) and Sc(40 nm)/CrN_x(1 nm)/Be(1 nm) (c), (d) systems.

from the CrN_x even more intense in this system and the ratio of metallic chromium to CrN_x is 3:1 (2.9) in this case. It is also seen that the beryllium layer somewhat protects the thin CrN_x layer from the oxidation in the environment. One can assume that beryllium, while protecting the CrN_x film from oxidation in the environment, allows nitrogen to be scavenged more freely; oxygen to some extent resists nitrogen scavenging.

The analysis of the Sc 2p line confirms the fairly strong scavenging of nitrogen from the CrN_x layer in this case. Attention is drawn to the significant intensity of the nitrogen peak in this case, which is due to the presence of contributions from both CrN_x and ScN_x compounds in this line.

It can be concluded that, depending on the sequence of deposition of layers in the system Sc/CrN_x, nitrogen is scavenged from chromium by scandium to one degree or another. In the case of CrN_x/Sc system, a net scavenging of nitrogen is observed, while in the Sc/CrN_x system the interaction of scandium with nitrogen gas before chromium layer deposition with formation of some amount of ScN_x is added.

Fig. 5 demonstrates the spectra collected from the Cr(39 nm)/ScN_x(2 nm) and ScN_x(40 nm)/Cr(1 nm)/Be(1 nm) systems. In these systems the scandium layer is nitridated. The main difference between these systems and systems with chromium nitridated layer is the absence of chromium nitride in the Cr 2p spectra; chromium does not interact with environment nitrogen during the deposition of first atoms of the ScN_x layer, and does not draw nitrogen from the scandium nitrided layer. A small amount of the chromium oxide and chromium hydroxide can be traced in the Cr 2p spectra of the Cr/ScN_x system and only a trace of the oxide in the Cr 2p spectrum of the ScN_x/Cr/Be system can be established. Sc 2p spectrum of the Cr/ScN_x system correlates well with the spectrum of the reference ScN_x film.

3.4. Theoretical predictions of nitridation effect

Since one of the applications of this system is the development of multilayer systems for X-ray optics, the question arises of the effect of nitridation of scandium and/or chromium layers on the peak reflection coefficients of the Cr/Sc mirror in the energy range of the "water transparency window". For this purpose, the reflection coefficients for structures containing nitrogen were calculated: CrN_x/Sc, Cr/ScN_x, CrN_x/ScN_x. For each pair of materials, such a ratio of thicknesses was chosen that is optimal for the considered energy. The optimal ratio was also estimated based on the formula from work [73]. Three materials were considered as chromium nitrides: Cr_2N, CrN, CrN_2. The density values for the first two materials were taken from the [67] and for the third one from the [74]. Only the ScN compound was used as scandium nitride, the density for which was taken from the [74]. The density and thickness ratio values used are presented in Table 1.

The spectral dependences R(E) were calculated at a normal angle of 0° (Fig. 6), a fixed number of layers N = 300, and a period d = 1.561 nm. Only the materials of the layers were varied. The layer thickness ratios

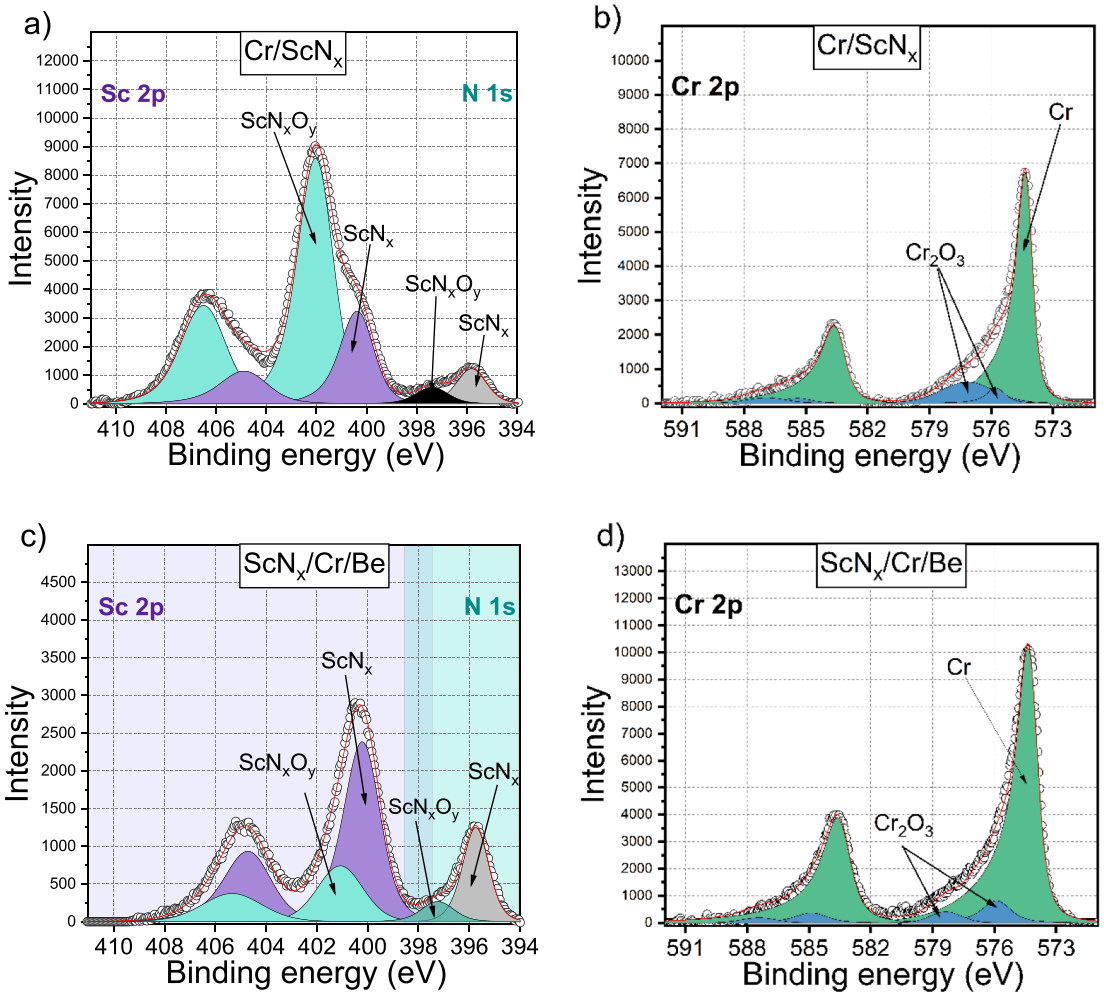

Fig. 5. Experimental and decomposed Sc 2p + N1s and Cr 2p photoelectron spectra collected from the Cr(39 nm)/ScN_x(2 nm) (a, b) and ScNx(40 nm)/Cr(1 nm)/Be (1 nm) (c, d) systems.

Table 1
Values of densities of the materials and ratios thickness of absorber to period width in mirrors.

Material	Density, g/cm^3
Sc	2.99
Cr	7.15
Cr_2N	6.8
CrN	5.9
CrN_2	5.09
ScN	4.27

Mirror	Optimal $d_{absorber}/d$
Cr/Sc	0.41
Cr_2N/Sc	0.43
CrN/Sc	0.45
CrN_2/Sc	0.48
Cr/Sc	0.41
Cr/ScN	0.43

calculated for an energy of 397 eV were used. The calculations were carried out using the IMD program [75].

As follows from the presented results, at a fixed number of pairs of layers, scandium nitridation negatively affects reflection, while chromium nitridation, on the contrary, can lead to an increase in reflection, and the more nitrogen in the compound, the better. Consider the effect of roughness/diffusion on reflection (Fig. 7). Let us try to understand the dependence of the degree of reduction of the peak reflection coefficient on the roughness/diffusion (σ) for different mirrors. Only three mirrors will be taken into account: Cr/Sc, CrN_2/Sc, and CrN_2/ScN. We will add the σ parameter as symmetrical (σ(Cr-on-Sc) = σ(Sc-on-Cr)), set the surface roughness to 0.

It can be seen that as the roughness/interdiffusion increases, the peak reflection coefficient decreases slightly faster for multilayer structures that contain nitrogen. The more nitrogen, the faster the decline. After σ = 0.3 nm, the benefit of using CrN_2 almost disappears, while the use of Cr_2N instead of Cr remains better up to σ = 0.5 nm. An analysis of the data obtained allows us to conclude that: i) structures with chromium nitride can have higher reflection coefficients compared to "pure" Cr/Sc; ii) in order for roughness/interdiffusion to reduce the peak reflectance slightly less, it is necessary to use chromium with a low nitrogen content; iii) it is necessary to exclude the formation of scandium nitrides.

3.5. $[Sc/CrN_x]_{300}$ before and after annealing

Taking into account the theoretical analysis of the effect of nitridation of the system, as well as detailed analysis of the processes at the interface between chromium and scandium, depending on the sequence of deposition of layers and nitriding of chromium and/or scandium, we consider a multilayer system $[Sc/CrN_x]_{300}$ synthesized in an argon + nitrogen (3%) medium. In the case of a multilayer system with thin layers, when using an energy of exciting photons of 1486.6 eV, several periods of the system are involved in the formation of a photoelectronic signal, which means that both the Sc/CrN_x and the CrN_x/Sc interfaces are involved in the process. As a result, the spectrum displays the sum signal due to the presence of both interfaces. As noted above, in the Sc/CrN_x-based system, as a result of the deposition of both scandium on CrN_x layer and CrN_x on scandium layer, the nitrogen is scavenged from chromium by scandium, but in the case of the succession of CrN_x on scandium layer, an additional contribution from the ScN_x compound is added as a result of the interaction of first scandium atoms with nitrogen. The presence of the intense nitrogen line in the N 1s spectrum (Fig. 8), which accumulates lines originated from ScN_x and CrN_x, reflects these processes. Rather intense Sc 2p line can be assigned to ScN_x. Also, small intensity lines originating from the metallic scandium and oxynitride scandium can be traced in the Sc 2p + N 1s spectrum. It should be noted that the positions of the peaks of metallic scandium and ScN_x coincide with the positions of analogous peak in the spectra of all the

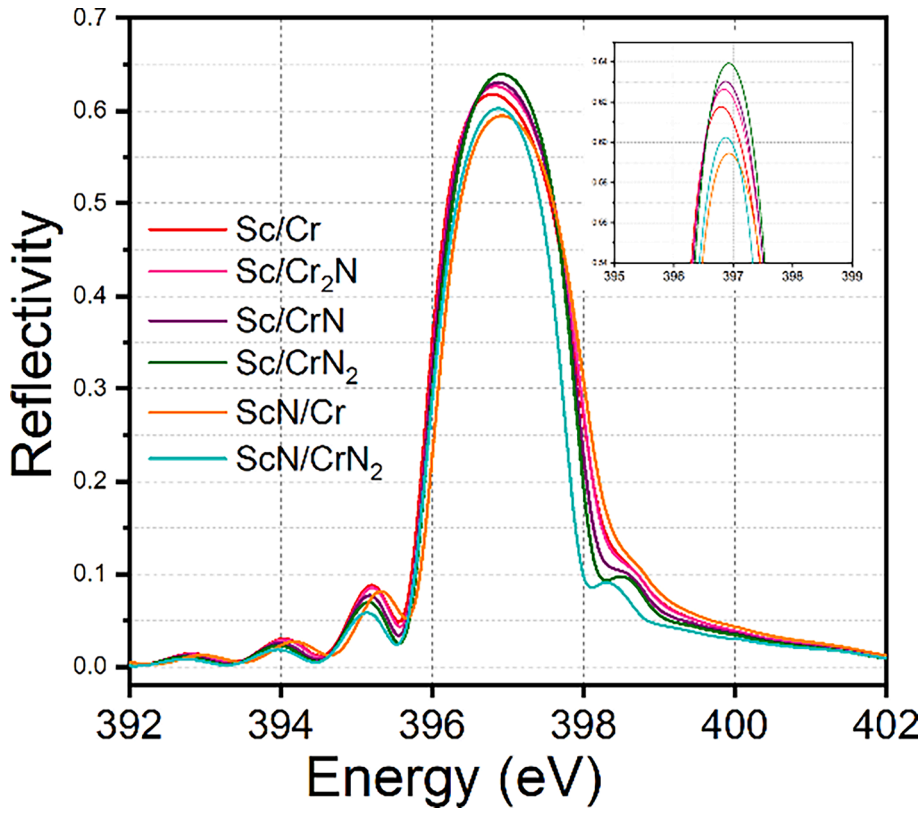

Fig. 6. The spectral dependences R(E) calculated at a normal angle of 0°, a fixed number of layers N = 300, and a period d = 1.561 nm for different mirrors.

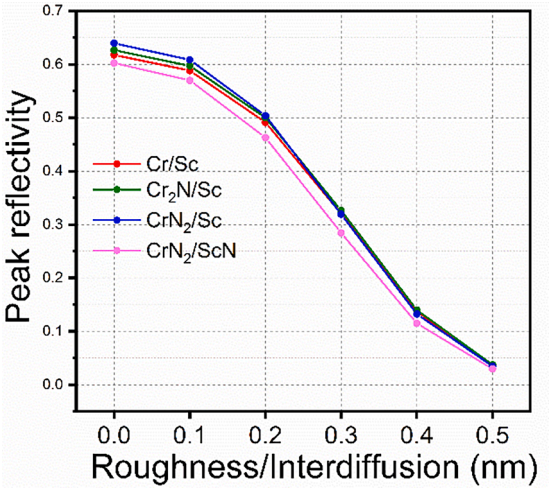

Fig. 7. Dependence of peak reflectivity on roughness/interdiffusion (σ) value.

above referenced samples. At the same time, the ScN_xO_y peak (401.0 eV) is shifted towards lower energies, not only relative to the ScNx film (402.5 eV), but also relative to Sc/N_2 film (401.8 eV). It is plausible to assume the highest nitriding of Sc in the multilayer system.

Analysis of Cr 2p spectrum reveals two main peaks comparable in intensity, which can be attributed to metallic chromium and CrN_x. The high intensity of the metallic chromium line is an additional confirmation of the active scavenging of nitrogen from the CrN_x layers. It is interesting to turn to the $Sc/CrN_x/Be$ system again. Only a small intensity CrNx line was traced in the Cr 2p spectrum of the $Sc/CrN_x/Be$ system. When considering the spectra of this system, it was suggested that oxygen to some extent resists nitrogen scavenging. The Cr 2p spectrum of multilayer system fully confirms this assumption.

An additional confirmation of this prediction was obtained during annealing of all studied samples. Effect of annealing depending on its temperature (250 °C, 350 °C, 450 °C) on the structure of all the studied samples was analyzed. As an example, the spectra of the multilayer system $[Sc/CrN_x]_{300}$ are shown in the Fig. 9. The main conclusion following from the analysis of the spectra is that during annealing, both layers, regardless of the sequence of deposition and nitriding of scandium or chromium, are oxidized to one degree or another. Minor increase in the dip in the region of 397.7 eV and the minor change in the high-energy edge of the broad peak located at an energy of about 395.5 eV upon annealing to 350 °C (Fig. 9a) indicates a slight decrease in the contribution of ScN_x content and the growth of scandium oxynitride that correlates well with a slight increase in the CrN_x contribution in the Cr 2p spectrum. During further annealing, the shape of the spectra is retained.

In general, it can be said that the shape of the spectrum is practically preserved during annealing, which means that annealing does not provoke further nitrogen scavenging from the CrN_x layer; actually, further mixing of scandium and CrN_x layers. Note that despite the preservation of the shape of the spectra, an increase in the oxide component is

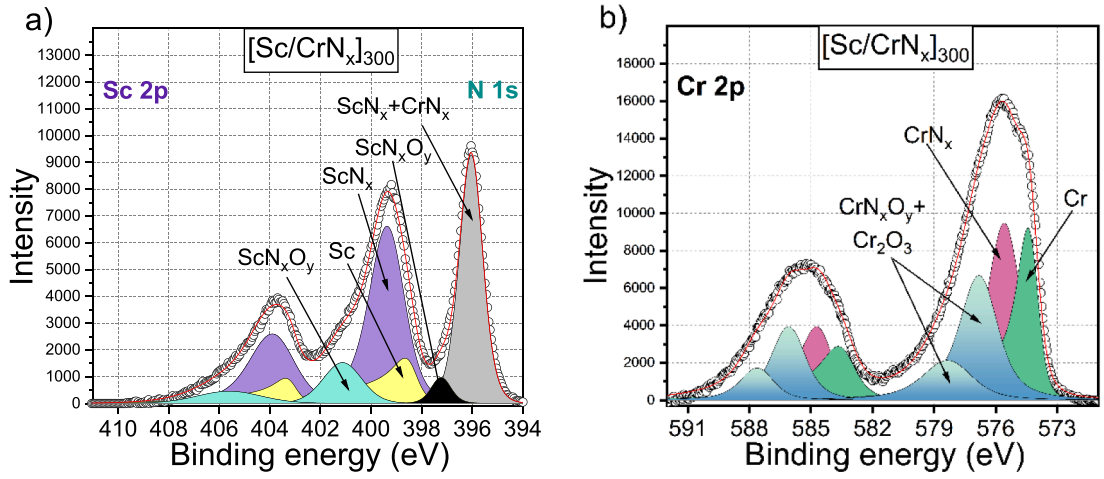

Fig. 8. Experimental and decomposed Sc 2p + N1s and Cr 2p photoelectron spectra collected from the multilayer system $[Sc/CrN_x]_{300}$.

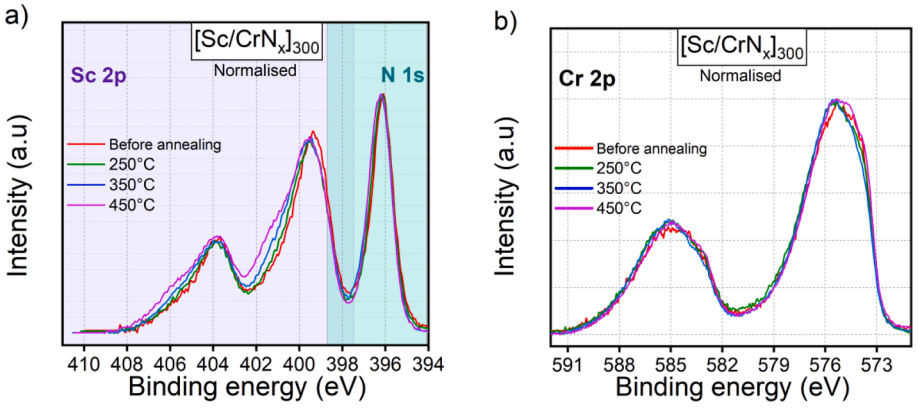

Fig. 9. Experimental and decomposed Sc 2p + N1s and Cr 2p photoelectron spectra collected from the reference system Sc(40 nm)/CrN_x(1 nm)/Be(1 nm) and multilayer system $[Sc/CrN_x]_{300}$ and annealed at temperatures 250 °C, 350 °C, 450 °C.

observed. Thus, it can be argued that the presence of oxygen and its gradual increase with increasing temperature prevents mixing of the layers in the system under consideration during annealing.

Comparing the multilayer system $[Sc/CrN_x]_{300}$ studied by us with the previously studied $[Sc/Cr]_{300}$ system [48], it can be argued that the nitriding of the chromium layer makes it possible to obtain a system resistant to annealing. This system is characterized by scandium scavenging of nitrogen from the CrN_x layer with the final formation of a predominantly nitrided scandium layer with a small contribution of metallic scandium. The second layer consists of approximately equal proportions of metallic chromium and CrN_x layers. Such a system is very resistant to elevated temperatures up to 450 °C.

3.6. X-ray reflectometry studies

X-ray reflection curves obtained for the $Si/[Sc/CrN_x]_{300}$ multilayer structure before and after annealing are shown in the Fig. 10. As can be seen from the figure, all curves correlate well with each other in shape, all comprise Bragg peak, which indicates the persistence of the layered structure in the $Si/[Sc/CrN_x]_{300}$ system. The annealing retains a significant intensity Bragg peak but with growth of the temperature of annealing a shift towards larger angles relative to the as-deposited sample can be traced that corresponds to a decrease in the multilayer period. Detailed analysis of the shape of all four peaks reveals a slight narrowing of the peak as a result of annealing and practically the preservation of its half-width at all annealing temperatures. X-ray diffraction data (Figure S1) showed that sample consists of X-ray amorphous layers, the crystallinity of which practically does not change with increasing temperature. In addition, the redistribution of the intensities of the higher-order Bragg peaks indicates that the d_{CrN}/d ratio also changes. The results show good thermal stability of the $[Sc/CrN_x]_{300}$ multilayer system. Noteworthy, a "pure" Cr/Sc multilayer was fully degraded after annealing at a temperature of 450 °C [48].

4. Conclusions

The effect of nitridation of Cr or Sc layer in the ultrathin multilayer structure Sc/Cr on the intermixing of the Cr and Sc layers was considered in details. To understand the physical mechanism underlying the interaction of chromium and scandium with nitrogen the passivation process by nitrogen was further considered. It was concluded that scandium actively interacts with nitrogen, regardless of the moment of nitrogen injection in the synthesis chamber. A comparison of the spectra of Sc/N_2 and ScN_x indicates the interaction of nitrogen with scandium layer, leading to the formation of ScN_x in both cases, while retaining a sufficient amount of metallic scandium only in the Sc/N_2. In contrast to scandium, the chromium layer does not interact with nitrogen at all during passivation. We found that a small amount of nitrogen is sufficient to improve the properties of the chromium layer during nitridation. It is small amounts of nitrogen that make it possible to preserve the amorphous structure in Sc/Cr structure, while according to existing researches, high nitrogen contents (more than 30%) inevitably cause crystallization of the layers.

A detailed sequential study of the interface depending on the deposition order of nitrided layers made it possible to establish the fact that scandium scavenged the nitrogen from the chromium layer. It was established that a net scavenging of nitrogen is observed in the case of CrN_x/Sc system, while in the Sc/CrN_x system the interaction of scandium with nitrogen gas before chromium layer deposition with formation of some amount of ScN_x is added.

The theoretical analysis of the effect of nitridation of the system was realized. Based on a joint analysis of theoretical data and experimental results, a $[Sc/CrN_x]_{300}$ multilayer system synthesized in an argon + nitrogen (3%) medium was prepared and studied at different annealing temperatures. Consideration of the spectra of this system allows one to suggest that oxygen to some extent resists nitrogen scavenging. This conclusion was supported by the results obtained during annealing of all studied samples.

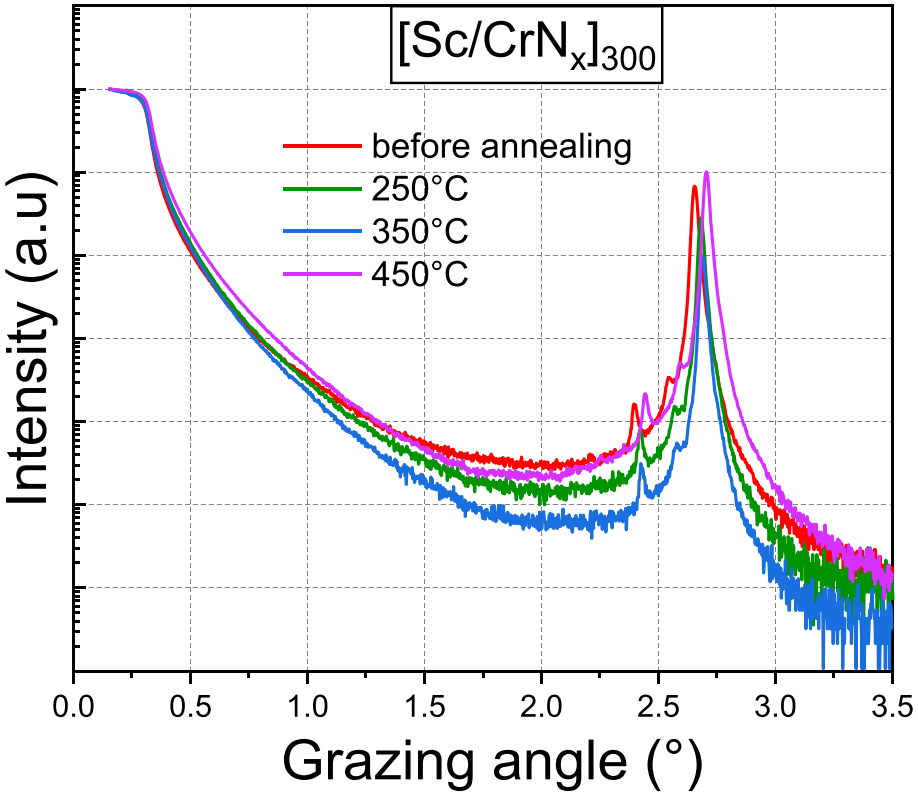

Fig. 10. X-ray reflection curves obtained for the $Si/[Sc/CrN_x]_{300}$ multilayer structure before and after annealing at 250 °C, 350 °C and 450 °C.

Analysis of the refection curves and diffraction patten indicates the persistence of the layered structure in the Si/[Sc/CrN_x]$_{300}$ system after annealing. A shift of the first Bragg peak towards larger angles relative to the as-deposited sample corresponds to a decrease in the multilayer period. According to the diffraction data the sample consists of X-ray amorphous layers, the crystallinity of which practically does not change with increasing temperature. It can be concluded that, in contrast to our previous study of the influence of the barrier layers on the thermal stability of the Sc/Cr multilayer system, the nitriding technique allows preserving the layered structure and the amorphousness of the layers up to 450 °C.

CRediT authorship contribution statement

E.O. Filatova: Supervision, Conceptualization, Writing – original draft. **S.S. Sakhonenkov:** Formal analysis, Investigation, Writing – review & editing. **A.V. Solomonov:** Formal analysis, Investigation, Writing – review & editing, Visualization. **R.M. Smertin:** Resources. **V. N. Polkovnikov:** Resources.

Declaration of Competing Interest

The authors declare that they have no known competing financial interests or personal relationships that could have appeared to influence the work reported in this paper.

Data availability

Data will be made available on request.

Acknowledgements

The work was supported by RSF grant 19-72-20125-П. The authors gratefully acknowledge Research Centers “Physical Methods of Surface Investigation”, “Centre for X-ray Diffraction Studies” of the Research Park, St. Petersburg State University, for the XPS and XRD data and National Research Center “Kurchatov Institute” for the providing access to the ESCA laboratory equipment and staff support.

Appendix A. Supplementary material

Supplementary data to this article can be found online at https://doi.org/10.1016/j.apsusc.2023.158791.

References

[1] V. V. Afanas’ev, A. Stesmans, L. Pantisano, S. Cimino, C. Adelmann, L. Goux, Y.Y. Chen, J.A. Kittl, D. Wouters, M. Jurczak, TiNx/HfO2 interface dipole induced by oxygen scavenging, Appl Phys Lett. 98 (2011) 132901. 10.1063/1.3570647.
[2] E.O. Filatova, A.S. Konashuk, F. Schaefers, V.V. Afanasev, Metallization-Induced Oxygen Deficiency of γ-Al2O3 Layers, J. Phys. Chem. C 120 (2016) 8979–8985, https://doi.org/10.1021/acs.jpcc.6b01352.
[3] L. Pantisano, V.V. Afanas’Ev, S. Cimino, C. Adelmann, L. Goux, Y.Y. Chen, J. A. Kittl, D. Wouters, M. Jurczak, Towards barrier height modulation in HfO2/TiN by oxygen scavenging - Dielectric defects or metal induced gap states? Microelectron Eng. 88 (2011) 1251–1254, https://doi.org/10.1016/j.mee.2011.03.057.
[4] L. Pantisano, T. Schram, B. O’Sullivan, T. Conard, S. De Gendt, G. Groeseneken, P. Zimmerman, A. Akheyar, M.M. Heyns, S. Shamuilla, V.V. Afanas’ev, A. Stesmans, Effective work function modulation by controlled dielectric monolayer deposition, Appl Phys Lett. 89 (2006) 2–5, https://doi.org/10.1063/1.2349310.
[5] F. De Stefano, V.V. Afanas’ev, M. Houssa, L. Goux, K. Opsomer, M. Jurczak, A. Stesmans, Modulation of electron barriers between TiNx and oxide insulators (SiO2, Al2O3) using Ti interlayer, Phys. Status Solidi A 211 (2014) 382–388, https://doi.org/10.1002/pssa.201330210.
[6] W. Mönch, Semiconductor Surfaces and Interfaces, Springer Series in Surface Sciences. (1993).
[7] C.G. Wang, T.H. Distefano, Polarization Layer at Metal/Insulator Interfaces, C R C Crit. Rev. Solid State Sci. 5 (1975) 327–335, https://doi.org/10.1080/10408437508243491.
[8] K.W. Lang N. D., Theory of metal surfaces: charge density and surface energy, Physical Review. (1970) 4555–4568.
[9] H.F. Dadgour, K. Endo, V.K. De, K. Banerjee, Grain-orientation induced work function variation in nanoscale metal-gate transistors - Part II: Implications for process, device, and circuit design, IEEE Trans Electron Devices. 57 (2010) 2515–2525, https://doi.org/10.1109/TED.2010.2063270.
[10] E.O. Filatova, A.S. Konashuk, S.S. Sakhonenkov, A.U. Gaisin, N.M. Kolomiiets, V. V. Afanas’ev, H.F.W. Dekkers, Mechanisms of TiN Effective Workfunction Tuning at Interfaces with HfO2and SiO2, J. Phys. Chem. C 124 (2020) 15547–15557, https://doi.org/10.1021/acs.jpcc.0c03605.
[11] I. Nedelcu, R.W.E. Van De Kruijs, A.E. Yakshin, F. Bijkerk, Temperature-dependent nanocrystal formation in Mo Si multilayers, Phys. Rev. B Condens. Matter. Mater. Phys. 76 (2007), https://doi.org/10.1103/PhysRevB.76.245404.
[12] A. Haase, V. Soltwisch, F. Scholze, S. Braun, Characterization of Mo/Si mirror interface roughness for different Mo layer thickness using resonant diffuse EUV scattering, in: A. Duparré, R. Geyl (Eds.), 2015: p. 962804. 10.1117/12.2191265.
[13] J.Z. Jiaoling Zhao, H.H. Hongbo He, H.W. Hu Wang, K.Y. Kui Yi, B.W. Bin Wang, and Y.C. and Yun Cui, Interface characterization of Mo/Si multilayers, Chinese Optics Letters. 14 (2016) 083401–083404. 10.3788/COL201614.083401.
[14] S. Braun, H. Mai, M. Moss, R. Scholz, A. Leson, Mo/Si multilayers with different barrier layers for applications as extreme ultraviolet mirrors, Japanese Journal of Applied Physics, Part 1: Regular Papers and Short Notes and Review Papers. 41 (2002) 4074–4081. 10.1143/JJAP.41.4074.
[15] S.A. Kasatikov, E.O. Filatova, S.S. Sakhonenkov, A.U. Gaisin, V.N. Polkovnikov, R. M. Smertin, Study of Interfaces of Mo/Be Multilayer Mirrors Using X-ray Photoelectron Spectroscopy, J. Phys. Chem. C 123 (2019) 25747–25755, https://doi.org/10.1021/acs.jpcc.9b07800.
[16] M.V. Svechnikov, N.I. Chkhalo, S.A. Gusev, A.N. Nechay, D.E. Pariev, A.E. Pestov, V.N. Polkovnikov, D.A. Tatarskiy, N.N. Salashchenko, F. Schäfers, M.G. Sertsu, A. Sokolov, Y.A. Vainer, M.V. Zorina, Influence of barrier interlayers on the performance of Mo/Be multilayer mirrors for next-generation EUV lithography, Opt Express. 26 (2018) 33718, https://doi.org/10.1364/oe.26.033718.
[17] S.S. Sakhonenkov, E.O. Filatova, S.A. Kasatikov, E.S. Fateeva, R.S. Pleshkov, V. N. Polkovnikov, Layer intermixing in ultrathin Cr/Be layered system and impact of barrier layers on interface region, Appl. Surf. Sci. 570 (2021), 151114, https://doi.org/10.1016/j.apsusc.2021.151114.
[18] A. Cavaleiro, J.T.M. de Hosson, Nanostructured coatings, (2006). https://research.rug.nl/en/publications/nanostructured-coatings (accessed September 6, 2023).
[19] J.-E. Sundgren, H.T.G. Hentzell, A review of the present state of art in hard coatings grown from the vapor phase, J. Vac. Sci. Technol. A 4 (1986) 2259–2279, https://doi.org/10.1116/1.574062.
[20] P.H. Mayrhofer, C. Mitterer, L. Hultman, H. Clemens, Microstructural design of hard coatings, Prog. Mater. Sci. 51 (2006) 1032–1114, https://doi.org/10.1016/j.pmatsci.2006.02.002.
[21] L. Hultman, Thermal stability of nitride thin films, Vacuum 57 (2000) 1–30, https://doi.org/10.1016/S0042-207X(00)00143-3.
[22] P. Patsalas, N. Kalfagiannis, S. Kassavetis, Optical Properties and Plasmonic Performance of Titanium Nitride, Materials 2015, Vol. 8, Pages 3128-3154. 8 (2015) 3128–3154. 10.3390/MA8063128.
[23] M.A. Moram, S. Zhang, ScGaN and ScAlN: emerging nitride materials, J Mater Chem A Mater. 2 (2014) 6042–6050, https://doi.org/10.1039/C3TA14189F.
[24] P.M. Mayrhofer, H. Riedl, H. Euchner, M. Stöger-Pollach, P.H. Mayrhofer, A. Bittner, U. Schmid, Microstructure and piezoelectric response of YxAl1−xN thin films, Acta Mater. 100 (2015) 81–89, https://doi.org/10.1016/J.ACTAMAT.2015.08.019.
[25] A. Zukauskaite, G. Wingqvist, J. Palisaitis, J. Jensen, P.O.A. Persson, R. Matloub, P. Muralt, Y. Kim, J. Birch, L. Hultman, Microstructure and dielectric properties of piezoelectric magnetron sputtered w-Sc xAl 1-xN thin films, J. Appl. Phys. 111 (2012) 93527, https://doi.org/10.1063/1.4714220/978760.
[26] P. Eklund, S. Kerdsongpanya, B. Alling, Transition-metal-nitride-based thin films as novel energy harvesting materials, J. Mater. Chem. C Mater. 4 (2016) 3905–3914, https://doi.org/10.1039/C5TC03891J.
[27] G. O’Sullivan, B. Li, P. Dunne, P. Hayden, D. Kilbane, R. Lokasani, E. Long, H. Ohashi, F. O’Reilly, J. Sheil, P. Sheridan, E. Sokell, C. Suzuki, E. White, T. Higashiguchi, Sources for beyond extreme ultraviolet lithography and water window imaging, Phys. Scr. 90 (2015) 54002, https://doi.org/10.1088/0031-8949/90/5/054002.
[28] H. Kumagai, Y. Tanaka, M. Murata, Y. Masuda, T. Shinagawa, Novel TiO2/ZnO multilayer mirrors at “water-window” wavelengths fabricated by atomic layer epitaxy, J. Phys. Condens. Matter 22 (2010), https://doi.org/10.1088/0953-8984/22/47/474008.
[29] B. Li, T. Higashiguchi, T. Otsuka, W. Jiang, A. Endo, P. Dunne, G. O’Sullivan, “Water window” sources: Selection based on the interplay of spectral properties and multilayer reflection bandwidth, Appl. Phys. Lett. 102 (2013) 1–5, https://doi.org/10.1063/1.4789982.
[30] D.H. Martz, M. Selin, O. von Hofsten, E. Fogelqvist, A. Holmberg, U. Vogt, H. Legall, G. Blobel, C. Seim, H. Stiel, H.M. Hertz, High average brightness water window source for short-exposure cryomicroscopy, Opt Lett. 37 (2012) 4425, https://doi.org/10.1364/ol.37.004425.
[31] G. Higashiguchi, Takeshi; Otsuka, Takamitsu; Yugami, Noboru; Endo, Akira; Li, Bowen; Dunne, Padraig; O’Sullivan, Feasibility study of efficient “water window” soft x-ray source, Am. Inst. Phys. 231503 (2012) 1201109.
[32] A. Guggenmos, R. Rauhut, M. Hofstetter, S. Hertrich, B. Nickel, J. Schmidt, E. M. Gullikson, M. Seibald, W. Schnick, U. Kleineberg, Aperiodic CrSc multilayer mirrors for attosecond water window pulses, Opt. Express. 21 (2013) 21728, https://doi.org/10.1364/oe.21.021728.

[33] I. Kopylets, O. Devizenko, E. Zubarev, V. Kondratenko, I. Artyukov, A. Vinogradov, O. Penkov, Short-Period Multilayer X-ray Mirrors for "Water" and "Carbon Windows" Wavelengths, J. Nanosci. Nanotechnol. 19 (2018) 518–531, https://doi.org/10.1166/jnn.2019.16471.

[34] T. Hatano, T. Ejima, T. Tsuru, Cr/Sc/Mo multilayer for condenser optics in water window microscopes, J. Electron. Spectros. Relat. Phenomena. 220 (2017) 14–16, https://doi.org/10.1016/j.elspec.2016.12.010.

[35] H. Legall, G. Blobel, H. Stiel, W. Sandner, C. Seim, P. Takman, D.H. Martz, M. Selin, U. Vogt, H.M. Hertz, D. Esser, H. Sipma, J. Luttmann, M. Höfer, H.D. Hoffmann, S. Yulin, T. Feigl, S. Rehbein, P. Guttmann, G. Schneider, U. Wiesemann, M. Wirtz, W. Diete, Compact x-ray microscope for the water window based on a high brightness laser plasma source, Opt. Express. 20 (2012) 18362, https://doi.org/10.1364/oe.20.018362.

[36] W. Ackermann, G. Asova, V. Ayvazyan, A. Azima, N. Baboi, J. Bähr, V. Balandin, B. Beutner, A. Brandt, A. Bolzmann, R. Brinkmann, O.I. Brovko, M. Castellano, P. Castro, L. Catani, E. Chiadroni, S. Choroba, A. Cianchi, J.T. Costello, D. Cubaynes, J. Dardis, W. Decking, H. Delsim-Hashemi, A. Delserieys, G. Di Pirro, M. Dohlus, S. Düsterer, A. Eckhardt, H.T. Edwards, B. Faatz, J. Feldhaus, K. Flöttmann, J. Frisch, L. Fröhlich, T. Garvey, U. Gensch, C. Gerth, M. Görler, N. Golubeva, H.J. Grabosch, M. Grecki, O. Grimm, K. Hacker, U. Hahn, J.H. Han, K. Honkavaara, T. Hott, M. Hüning, Y. Ivanisenko, E. Jaeschke, W. Jalmuzna, T. Jezynski, R. Kammering, V. Katalev, K. Kavanagh, E.T. Kennedy, S. Khodyachykh, K. Klose, V. Kocharyan, M. Körfer, M. Kollewe, W. Koprek, S. Korepanov, D. Kostin, M. Krassilnikov, G. Kube, M. Kuhlmann, C.L.S. Lewis, L. Lilje, T. Limberg, D. Lipka, F. Löhl, H. Luna, M. Luong, M. Martins, M. Meyer, P. Michelato, V. Miltchev, W.D. Möller, L. Monaco, W.F.O. Müller, O. Napieralski, O. Napoly, P. Nicolosi, D. Nölle, T. Nüez, A. Oppelt, C. Pagani, R. Paparella, N. Pchalek, J. Pedregosa-Gutierrez, B. Petersen, B. Petrosyan, G. Petrosyan, L. Petrosyan, J. Pflüger, E. Plönjes, L. Poletto, K. Pozniak, E. Prat, D. Proch, P. Pucyk, P. Radcliffe, H. Redlin, K. Rehlich, M. Richter, M. Roehrs, J. Roensch, R. Romaniuk, M. Ross, J. Rossbach, V. Rybnikov, M. Sachwitz, E.L. Saldin, W. Sandner, H. Schlarb, B. Schmidt, M. Schmitz, P. Schmüser, J.R. Schneider, E. A. Schneidmiller, S. Schnepp, S. Schreiber, M. Seidel, D. Sertore, A.V. Shabunov, C. Simon, S. Simrock, E. Sombrowski, A.A. Sorokin, P. Spanknebel, R. Spesyvtsev, L. Staykov, B. Steffen, F. Stephan, F. Stulle, H. Thom, K. Tiedtke, M. Tischer, S. Toleikis, R. Treusch, D. Trines, I. Tsakov, E. Vogel, T. Weiland, H. Weise, M. Wellhöfer, M. Wendt, I. Will, A. Winter, K. Wittenburg, W. Wurth, P. Yeates, M. V. Yurkov, I. Zagorodnov, K. Zapfe, Operation of a free-electron laser from the extreme ultraviolet to the water window, Nat. Photonics. 1 (2007) 336–342, https://doi.org/10.1038/nphoton.2007.76.

[37] A. Lapresta-Fernández, A. Salinas-Castillo, S. Anderson De La Llana, J.M. Costa-Fernández, S. Domínguez-Meister, R. Cecchini, L.F. Capitán-Vallvey, M.C. Moreno-Bondi, M.P. Marco, J.C. Sánchez-López, I.S. Anderson, A general perspective of the characterization and quantification of nanoparticles: Imaging, spectroscopic, and separation techniques, Crit. Rev. Solid State Mater. Sci. 39 (2014) 423–458, https://doi.org/10.1080/10408436.2014.899890.

[38] B.E. Van Kuiken, H. Cho, K. Hong, M. Khalil, R.W. Schoenlein, T.K. Kim, N. Huse, Time-Resolved X-ray Spectroscopy in the Water Window: Elucidating Transient Valence Charge Distributions in an Aqueous Fe(II) Complex, J. Phys. Chem. Lett. 7 (2016) 465–470, https://doi.org/10.1021/acs.jpclett.5b02509.

[39] F. Eriksson, G.A. Johansson, H.M. Hertz, E.M. Gullikson, U. Kreissig, J. Birch, 14.5% near-normal incidence reflectance of Cr/Sc x-ray multilayer mirrors for the water window, Opt. Lett. 28 (2003) 2494, https://doi.org/10.1364/OL.28.002494.

[40] F. Schäfers, S.A. Yulin, T. Feigl, N. Kaiser, At-wavelength metrology on Sc-based multilayers for the UV and water window, in: A. Duparre, B. Singh (Eds.), Proceedings of SPIE, 2003: p. 138. 10.1117/12.505695.

[41] M. Prasciolu, A.F.G. Leontowich, K.R. Beyerlein, S. Bajt, Thermal stability studies of short period Sc/Cr and Sc/B4C/Cr multilayers, Appl. Opt. 53 (2014) 2126, https://doi.org/10.1364/AO.53.002126.

[42] N. Ghafoor, F. Eriksson, E. Gullikson, L. Hultman, J. Birch, Incorporation of nitrogen in Cr/Sc multilayers giving improved soft x-ray reflectivity, Appl. Phys. Lett. 92 (2008), 091913, https://doi.org/10.1063/1.2857459.

[43] T. Kuhlmann, S. Yulin, T. Feigl, N. Kaiser, T. Gorelik, U. Kaiser, W. Richter, Chromium–scandium multilayer mirrors for the nitrogen Kα line in the water window region, Appl. Opt. 41 (2002) 2048, https://doi.org/10.1364/AO.41.002048.

[44] C. Burcklen, S. de Rossi, E. Meltchakov, D. Dennetière, B. Capitanio, F. Polack, F. Delmotte, High-reflectance magnetron-sputtered scandium-based x-ray multilayer mirrors for the water window, Opt. Lett. 42 (2017) 1927, https://doi.org/10.1364/ol.42.001927.

[45] N. Ghafoor, F. Eriksson, A.S. Mikhaylushkin, I.A. Abrikosov, M. Eric, U. Gullikson, M. Kressig, L. Beckers, J.B. Hultman, Effects of O and N impurities on the nanostructural evolution during growth of Cr/Sc multilayers, J. Mater. Res. 24 (2009) 79–95, https://doi.org/10.1557/JMR.2009.0004.

[46] F. Eriksson, N. Ghafoor, L. Hultman, J. Birch, Reflectivity and structural evolution of Cr/Sc and nitrogen containing Cr/Sc multilayers during thermal annealing, J. Appl. Phys. 104 (2008), https://doi.org/10.1063/1.2980051.

[47] N. Ghafoor, F. Eriksson, A. Aquila, E. Gullikson, F. Schäfers, G. Greczynski, J. Birch, Impact of B4C co-sputtering on structure and optical performance of Cr/Sc multilayer X-ray mirrors, Opt. Express. 25 (2017) 18274, https://doi.org/10.1364/OE.25.018274.

[48] E.O. Filatova, S.S. Sakhonenkov, A.V. Solomonov, R.M. Smertin, V.N. Polkovnikov, Refined thermal stability of Cr/Sc multilayers with Si(Be) barrier layers, Appl. Surf. Sci. 611 (2023), https://doi.org/10.1016/j.apsusc.2022.155743.

[49] V.N. Polkovnikov, N.N. Salashchenko, M.V. Svechnikov, N.I. Chkhalo, Beryllium-based multilayer X-ray optics, Phys. Usp. 63 (2020) 83–95, https://doi.org/10.3367/UFNe.2019.05.038623.

[50] N. Chkhalo, A. Lopatin, A. Nechay, D. Pariev, A. Pestov, V. Polkovnikov, N. Salashchenko, F. Schäfers, M. Sertsu, A. Sokolov, S. Mikhail, T. Nikolay, Z. Sergey, Beryllium-Based Multilayer Mirrors and Filters for the Extreme Ultraviolet Range, J. Nanosci. Nanotechnol. 19 (2019) 546–553, https://doi.org/10.1166/jnn.2019.16474.

[51] S. Tougaard, Universality classes of inelastic electron scattering cross-sections, Surface Interface Anal. 25 (1997) 137–154, https://doi.org/10.1002/(SICI)1096-9918(199703)25:3<137::AID-SIA230>3.0.CO;2-L.

[52] M.C. Biesinger, L.W.M. Lau, A.R. Gerson, R.St.C. Smart, Resolving surface chemical states in XPS analysis of first row transition metals, oxides and hydroxides: Sc, Ti, V, Cu and Zn, Appl. Surf. Sci. 257 (2010) 887–898, https://doi.org/10.1016/j.apsusc.2010.07.086.

[53] J. Baltrusaitis, P.M. Jayaweera, V.H. Grassian, XPS study of nitrogen dioxide adsorption on metal oxide particle surfaces under different environmental conditions, PCCP 11 (2009) 8295–8305, https://doi.org/10.1039/b907584d.

[54] A. Le Febvrier, N. Tureson, N. Stilkerich, G. Greczynski, P. Eklund, Effect of impurities on morphology, growth mode, and thermoelectric properties of (1 1 1) and (0 0 1) epitaxial-like ScN films, J. Phys. D Appl. Phys. 52 (2019), https://doi.org/10.1088/1361-6463/aaeb1b.

[55] V. Maurice, W.P. Yang, P. Marcus, XPS and STM Investigation of the Passive Film Formed on Cr(110) Single-Crystal Surfaces, J. Electrochem. Soc. 141 (1994) 3016–3027, https://doi.org/10.1149/1.2059274/XML.

[56] DavidR. Rosseinsky, GeraldK. Muthakia, ColinL. Honeybourne, RichardJ. Ewen, Novel chromium(III)/(VI) adducts of XPS-determined mixed valence, from electroreduced chromium(VI), Transition Metal Chemistry. 20 (1995). 10.1007/BF00135410.

[57] E. Kemnitz, A. Kohne, I. Grohmann, A. Lippitz, W.E.S. Unger, X-Ray Photoelectron and X-Ray Excited Auger Electron Spectroscopic Analysis of Surface Modifications of Chromia during Heterogeneous Catalyzed Chlorine/Fluorine Exchange, J. Catal. 159 (1996) 270–279, https://doi.org/10.1006/JCAT.1996.0088.

[58] X.Y. Li, E. Akiyama, H. Habazaki, A. Kawashima, K. Asami, K. Hashimoto, An XPS study of passive films on corrosion-resistant Cr·Zr alloys prepared by sputter deposition, Corros. Sci. 39 (1997) 1365–1380, https://doi.org/10.1016/S0010-938X(97)00035-8.

[59] T. Mega, K. Takao, J. Shimomura, State analysis of electrolytic chromate film by XPS and SXS, Appl. Surf. Sci. 121–122 (1997) 120–124, https://doi.org/10.1016/S0169-4332(97)00269-9.

[60] N.S. McIntyre, T.C. Chan, C. Chen, Characterization of oxide structures formed on nickel-chromium alloy during low pressure oxidation at 500–600°C, Oxid. Met. 33 (1990) 457–479, https://doi.org/10.1007/BF00666809/METRICS.

[61] I. Grohmann, E. Kemnitz, A. Lippitz, W.E.S. Unger, Curve fitting of Cr 2p photoelectron spectra of Cr2O3 and CrF3, Surface and Interface, Analysis 23 (1995) 887–891, https://doi.org/10.1002/sia.740231306.

[62] M.C. Biesinger, C. Brown, J.R. Mycroft, R.D. Davidson, N.S. McIntyre, X-ray photoelectron spectroscopy studies of chromium compounds, Surface Interface Anal. 36 (2004) 1550–1563, https://doi.org/10.1002/sia.1983.

[63] E. Ünveren, E. Kemnitz, S. Hutton, A. Lippitz, W.E.S. Unger, Analysis of highly resolved x-ray photoelectron Cr 2p spectra obtained with a Cr2O3 powder sample prepared with adhesive tape, Surface Interface Anal. 36 (2004) 92–95, https://doi.org/10.1002/SIA.1655.

[64] M.C. Biesinger, B.P. Payne, B.R. Hart, A.P. Grosvenor, N.S. McIntryre, L.W.M. Lau, R.S.C. Smart, Quantitative chemical state XPS analysis of first row transition metals, oxides and hydroxides, J. Phys. Conf. Ser. 100 (2008), 012025, https://doi.org/10.1088/1742-6596/100/1/012025.

[65] M.C. Biesinger, B.P. Payne, A.P. Grosvenor, L.W.M. Lau, A.R. Gerson, R.S.C. Smart, Resolving surface chemical states in XPS analysis of first row transition metals, oxides and hydroxides: Cr, Mn, Fe, Co and Ni, Appl. Surf. Sci. 257 (2011) 2717–2730, https://doi.org/10.1016/J.APSUSC.2010.10.051.

[66] A. Lippitz, T. Hübert, XPS investigations of chromium nitride thin films, Surf. Coat Technol. 200 (2005) 250–253, https://doi.org/10.1016/j.surfcoat.2005.02.091.

[67] CRC Handbook of Chemistry and Physics, 2009−2010, 90th ed., American Chemical Society, 2009. 10.1021/ja906434c.

[68] CasaXPS: Processing Software for XPS, AES, SIMS and More (Casa Software Ltd., Teignmouth), (n.d.). http://www.casaxps.com/.

[69] M.P. Seah, S.J. Spencer, Ultrathin SiO2 on Si IV. Intensity measurement in XPS and deduced thickness linearity, Surface Interface Anal. 35 (2003) 515–524, https://doi.org/10.1002/SIA.1565.

[70] S.S. Sakhonenkov, E.O. Filatova, Interface formation between Be and W layers depending on its thickness and ordering, Appl. Surf. Sci. 534 (2020), 147636, https://doi.org/10.1016/j.apsusc.2020.147636.

[71] B. Wang, E. Wu, Y. Wang, L. Xiong, S. Liu, Activation treatment effects on characteristics of BeO layer and secondary electron emission properties of an activated Cu-Be alloy, Appl. Surf. Sci. 355 (2015) 19–25, https://doi.org/10.1016/j.apsusc.2015.06.189.

[72] E.O. Wrasse, R.J. Baierle, First principles study of native defects in BeO, in: Phys Procedia, Elsevier B.V., 2012: pp. 79–83. 10.1016/j.phpro.2012.03.675.

[73] I.V. Kozhevnikov, A.V. Vinogradov, Multilayer x-ray mirrors, J. Russ. Laser Res. 16 (1995) 343–385, https://doi.org/10.1007/BF02581074.
[74] A. Jain, S.P. Ong, G. Hautier, W. Chen, W.D. Richards, S. Dacek, S. Cholia, D. Gunter, D. Skinner, G. Ceder, K.A. Persson, Commentary: The Materials Project: A materials genome approach to accelerating materials innovation, APL Mater. 1 (2013), 011002, https://doi.org/10.1063/1.4812323.
[75] D.L. Windt, IMD—Software for modeling the optical properties of multilayer films, Comput. Phys. 12 (1998) 360, https://doi.org/10.1063/1.168689.